

Submitted, accepted and published by:  
Chemical Engineering Journal 144 (2008) 289–298

# **Synthesis gas generation by chemical-looping reforming in a batch fluidized bed reactor using Ni- based oxygen carriers**

**Luis F. de Diego\*, María Ortiz, Juan Adánez, Francisco García-Labiano, Alberto  
Abad, and Pilar Gayán**

Department of Energy and Environment, Instituto de Carboquímica (C.S.I.C.)

Miguel Luesma Castán 4, 50018 Zaragoza, Spain

Phone number: +34 976 733 977

Fax number: +34 976 733 318

E-mail: [ldediego@icb.csic.es](mailto:ldediego@icb.csic.es)

\*Corresponding Author. Tel.: +34-976-733977; Fax: +34-976-733318; *E-mail address*:  
[ldediego@icb.csic.es](mailto:ldediego@icb.csic.es) (L.F. de Diego)

## **Abstract**

Chemical-looping reforming (CLR) utilizes the same basic principles as Chemical-looping combustion (CLC), being the main difference that the wanted product in CLR is H<sub>2</sub> and CO. Therefore, in the CLR process the air to fuel ratio is kept low to prevent the complete oxidation of the fuel to CO<sub>2</sub> and H<sub>2</sub>O.

Ni-based oxygen carriers prepared by impregnation on alumina have been studied in a thermogravimetric analyzer (TGA) and in a batch fluidized bed reactor in order to know

its potential for CLR of CH<sub>4</sub>. In the TGA the reactivity of the oxygen carriers has been determined. In the batch fluidized bed the effect on the gas product distribution produced during reduction/oxidation cycles and on the carbon deposition of different operating conditions, as type of support, reaction temperature, H<sub>2</sub>O/CH<sub>4</sub> molar ratio, and preparation method, has been tested and analyzed.

It was found that the support (different types of alumina) used to prepare the oxygen carriers had an important effect on the reactivity of the oxygen carriers, on the gas product distribution, and on the carbon deposition. In addition, for all oxygen carriers prepared, an increase in the reaction temperature and/or in the H<sub>2</sub>O/CH<sub>4</sub> molar ratio produced a decrease in the carbon deposition during the reduction period. Finally, it was observed that the oxygen carriers prepared by a deposition-precipitation method had higher tendency to increase the C deposition than the oxygen carriers prepared by dry impregnation.

## **1. Introduction**

Catalytic reforming of CH<sub>4</sub>, natural gas or light hydrocarbons is a commercial process to produce synthesis gas, which is the main source for the production of ammonia, methanol, hydrogen, and many other important products. At the present, steam reforming of natural gas, where the reforming takes place in reactor tubes packed with catalyst, is the most important method for synthesis gas production. However, important developments in processes, in equipment designs, and in catalysts used are constantly been made [1-3].

Chemical-looping combustion (CLC) is a novel combustion technology with inherent separation of the greenhouse gas CO<sub>2</sub> that involves the use of an oxygen carrier, which

transfers oxygen from air to the fuel avoiding the direct contact between them. CLC system is made of two interconnected reactors, designated as air and fuel reactors. In the fuel reactor, the fuel gas ( $C_nH_{2m}$ ) is oxidized to  $CO_2$  and  $H_2O$  by a metal oxide (MeO) that is reduced to a metal (Me) or a reduced form of MeO. The metal or reduced oxide is further transferred into the air reactor where it is oxidized with air, and the material regenerated is ready to start a new cycle. The flue gas leaving the air reactor contains  $N_2$  and unreacted  $O_2$ . The exit gas from the fuel reactor contains only  $CO_2$  and  $H_2O$ . After water condensation, almost pure  $CO_2$  can be obtained with little energy lost for component separation.

As shown in Figure 1, chemical-looping reforming (CLR) utilizes the same basic principles as CLC, being the main difference that the wanted product in CLR are not heat but  $H_2$  and CO. Therefore, in the CLR process the air to fuel ratio is kept low to prevent the complete oxidation of the fuel to  $CO_2$  and  $H_2O$ . An important aspect to be considered in a CLR system is the heat balance. The oxidation reaction of the metal oxide is very exothermic, however, the reduction reactions are endothermic. So, the heat for the endothermic reduction reactions is given by the circulating solids coming from the air reactor at higher temperature. The heat generated in the air reactor must be enough high to fulfil the heat balance in the system.

CLR, as described in Figure 1, was proposed by Mattisson et al. [4]. These authors [5] examined the thermodynamics and the heat balance of the fuel and air reactors using  $CuO/SiO_2$  and  $NiO/SiO_2$  as oxygen carriers and found that, in order to maintain a high temperature and  $CH_4$  conversion, the fraction of oxygen supplied by the steam should not exceed approximately 0.3 of the total oxygen added to the fuel reactor. In addition, they found that the selectivity towards  $H_2$  production was higher with the  $NiO/SiO_2$  oxygen carrier than with the  $CuO/SiO_2$  oxygen carrier.

Zafar et al. [6] prepared and tested in a laboratory fluidized bed reactor different oxygen carriers consisting of oxides of Fe, Mn, Ni and Cu supported on SiO<sub>2</sub>. They observed that the oxygen carriers based on Ni- and Cu- showed the highest reactivity, but only the NiO/SiO<sub>2</sub> showed high selectivity toward H<sub>2</sub>. Some carbon deposition was found on the oxygen carriers of Mn, Cu and Ni during the reduction period, and considerable reactivity deactivation as a function of the cycle was observed for the Ni, Fe, and Mn based carriers working at 950 °C. This was attributed to the formation of metal silicates, which do not react at a sufficient rate. Zafar et al. [7 ] also studied oxides of Ni, Cu, Fe and Mn supported on SiO<sub>2</sub> and MgAl<sub>2</sub>O<sub>4</sub> in a thermogravimetric analyzer (TGA). Working with SiO<sub>2</sub> as support they found similar results that those obtained in the fluidized bed, however they found that Fe and Mn oxides supported on MgAl<sub>2</sub>O<sub>4</sub> showed a rather high reactivity during reduction and oxidation and can be possibly used in the CLR process.

Ryden et al. [8] worked in a continuous laboratory reactor consisting of two interconnected fluidized beds with an oxygen carrier made of NiO and MgAl<sub>2</sub>O<sub>4</sub>. Complete conversion of natural gas was achieved and the selectivity towards H<sub>2</sub> and CO was high. Formation of solid carbon was noticed for some experiments with dry gas, but adding steam to natural gas the carbon formation was reduced or eliminated. These authors confirmed that the concept chemical-looping reforming is feasible and should be further investigated.

Although the same oxygen carriers are available for CLR and CLC, NiO appears the most interesting due to its strong catalytic properties. Metallic Ni is used in most commercial steam reforming catalyst.

In this work, Ni-based oxygen carriers prepared by impregnation on alumina have been studied in a TGA and in a batch fluidized bed reactor, in order to know its potential as

oxygen carriers for CLR. The main objective was to know the gas product distribution produced during the oxygen carrier reduction period and to determine the operating conditions that avoid or minimize carbon deposition. Different operating conditions, as reaction temperature, H<sub>2</sub>O/CH<sub>4</sub> molar ratio, type of carrier, and preparation method, has been tested and analyzed.

## **2. Experimental Section**

### **2.1 Materials**

The oxygen carriers used in the process are composed of a metal oxide as an oxygen source for the combustion process, and an inert as a binder for increasing the mechanical strength.

Commercial  $\gamma$ -Al<sub>2</sub>O<sub>3</sub> (Puralox NWA-155, Sasol Germany GmbH),  $\theta$ -Al<sub>2</sub>O<sub>3</sub> (obtained by calcination of  $\gamma$ -Al<sub>2</sub>O<sub>3</sub> at 1100 °C during 2 hours) and  $\alpha$ -Al<sub>2</sub>O<sub>3</sub> (obtained by calcination of  $\gamma$ -Al<sub>2</sub>O<sub>3</sub> at 1150 °C during 2 hours) particles of 0.1-0.32 mm, with densities of 1.3, 1.7 and 2.0 g/cm<sup>3</sup> and porosities of 55.4 %, 55.0 and 47.3 % respectively, were used as support to prepare oxygen carriers by dry impregnation. Ni-based oxygen carriers were prepared by addition of a volume of an aqueous solution of Ni(NO<sub>3</sub>)<sub>2</sub>·6H<sub>2</sub>O (>99.5 % Panreac) corresponding to the total pore volume of the support particles. The aqueous solution was slowly added to the alumina particles, with thorough stirring at room temperature. The desired active phase loading was achieved by applying successive impregnations followed by calcination at 550 °C, in air atmosphere for 30 min, to decompose the impregnated metal nitrates into insoluble metal oxide. Finally, the carriers were sintered for 1 h at 950 °C.

Two Ni-based oxygen carriers (using  $\gamma$ -Al<sub>2</sub>O<sub>3</sub> and  $\alpha$ -Al<sub>2</sub>O<sub>3</sub> as supports) were prepared by precipitation-deposition by changing the pH level of a nitrate solution [9]. Good distribution of high active metal content over the internal surface of the support was reported [9-10] using this method. Urea was used to increase the pH of the suspension to produce hydroxyl groups. The reaction, in which urea produce hydroxyl groups, exhibits a considerable rate only at temperatures above 60°C [10]. In this work, the precipitation was carried out keeping the suspension at 90°C for 20 h under stirring with a urea/Ni molar ratio of 1.9 (usually ratios are 1.5-2-5 times the amount theoretically needed). The resulting solid was filtered, thoroughly washed with distilled water and dried overnight at 100°C. Finally, the samples were calcined at 950 °C in a muffle for 1 h. The final metal content deposited in the sample was determined by analysis in an Inductive Coupled Plasma (ICP).

Table 1 shows all the oxygen carriers prepared. The samples were designated with the metal oxide followed by its weight content, and the inert used as support. These oxygen carriers were physically and chemically characterized by several techniques. The bulk density of the oxygen carrier particles was calculated weighting a known volume of solid and assuming that the void was 0.45 corresponding to loosely packed bed. The mechanical strength, determined using a Shimpo FGN-5X crushing strength apparatus, was taken as the average value of 20 measurements of the force needed to fracture a particle. Porosities were measured by Hg intrusion in a Quantachrome PoreMaster 33. The identification of crystalline chemical species was carried out by powder X-ray diffraction (XRD) patterns acquired in an X-ray diffractometer Bruker AXS D8ADVANCE using Ni-filtered Cu K $\alpha$  radiation equipped with a graphite monochromator. As can be observed in the table the oxygen carriers prepared using  $\gamma$ -Al<sub>2</sub>O<sub>3</sub> as support had lower density and mechanical strength than the oxygen carriers

prepared using  $\alpha$ -Al<sub>2</sub>O<sub>3</sub>. XRD patterns showed the formation of aluminium spinel compounds in the majority of the oxygen carriers.

## **2.2 Thermogravimetric Analyzer**

Multicycle tests to analyze the reactivity of the oxygen carriers during successive reduction-oxidation cycles were carried out in a TGA, CI Electronics type, described elsewhere [11-12]. For the experiments, the oxygen carrier was loaded in a platinum basket and heated to the set operating temperature in air atmosphere. After stabilization, the experiment started by exposing the oxygen carrier to alternating reducing and oxidizing conditions.

The reducing gas was saturated in water by bubbling it through a water containing saturator at the selected temperature to reach the desired water concentration. The composition of the gas selected for the reducing experiments was composed by 15 vol.% CH<sub>4</sub>, and 20 vol.% H<sub>2</sub>O (N<sub>2</sub> balance) and the gas used for oxidation was 100 vol.% air. To avoid mixing of combustible gas and air, nitrogen was introduced for two minutes after each reducing and oxidizing period. The experiments were carried out at temperatures up to 950 °C.

Temperature programmed reduction (TPR) tests were also performed in the TGA. A gas stream of 75 mL/minute containing 10 vol.% of H<sub>2</sub> in Ar was used as reducing gas. The temperature of the sample was raised from ambient to 1000 °C at a rate of 20°C/minute.

## **2.3 Fluidized Bed Reactor**

Reduction-oxidation multi-cycles were carried out in a fluidized bed reactor to know the gas product distribution during the reaction of an oxygen carrier in similar operating

conditions to that existing in a CLR process. The fluidization behaviour of the different materials with respect to agglomeration phenomena can be also observed.

Figure 2 shows the experimental set-up used for testing the oxygen carriers. It consisted of a system for gas feeding, a fluidized bed (FB) reactor, a two ways system to recover the solids elutriated from the FB, and a gas analysis system. The gas feeding system had different mass flow controllers for different gases and water. The FB reactor of 54 mm D.I. and 500 mm height, with a preheating zone just under the distributor, was fed with 300-400 g of oxygen carrier with a particle size of 0.1-0.3 mm. The entire system was inside an electrically heated furnace. The reactor had two connected pressure taps in order to measure the differential pressure drop in the bed. Agglomeration problems, causing defluidization of the bed, could be detected by a sharp decrease in the bed pressure drop during operation. Two hot filters located downstream from the FB recovered the solids elutriated from the bed during the successive reduction-oxidation cycles. Different gas analyzers continuously measured the gas composition at each time. The CO, CO<sub>2</sub>, H<sub>2</sub>O, and CH<sub>4</sub> gas concentrations were measured in two infrared analyzers (FTIR and NDIR), the O<sub>2</sub> concentration was measured in a paramagnetic analyzer, and the H<sub>2</sub> concentration was measured by gas conductivity.

The tests were carried out at 800-950°C with an inlet superficial gas velocity into the reactor of 0.15 m/s. The composition of the gas during reduction was 25vol% CH<sub>4</sub>, 7.5-17.5vol% H<sub>2</sub>O (H<sub>2</sub>O/CH<sub>4</sub> molar ratios of 0.3, 0.5, and 0.7) and the rest N<sub>2</sub>, and during oxidation 10-15vol% O<sub>2</sub> in N<sub>2</sub>. To avoid mixing of CH<sub>4</sub> and O<sub>2</sub>, N<sub>2</sub> was introduced for two minutes after each reducing and oxidizing period.



### 3. Results and discussion.

#### 3.1 Oxygen carrier reactivity in TGA.

TGA experiments allowed to analyze the reactivity of the oxygen carriers under well-defined conditions, and in the absence of complex fluidizing factors such as those derived from particle attrition and interphase mass transfer processes. For screening purposes, at least five cycles of reduction and oxidation were carried out with each carrier. The carriers usually stabilized after the first cycle, for which the reduction reaction rate was slower. The oxygen carrier reactivity corresponding to the cycle 5 was used for comparison purposes. Reactivity data were obtained in TGA tests from the weight variations during the reduction and oxidation cycles as a function of time. The oxygen carrier conversion was calculated as:

$$\text{For reduction: } X = \frac{m_{\text{ox}} - m}{m_{\text{ox}} - m_{\text{red}}} \quad (1)$$

$$\text{For oxidation: } X = 1 - \frac{m_{\text{ox}} - m}{m_{\text{ox}} - m_{\text{red}}} \quad (2)$$

where  $m$  is the mass of sample at a generic time,  $m_{\text{ox}}$  is the mass of the sample fully oxidized and  $m_{\text{red}}$  the mass of the sample in the reduced form.

The effect of the support on the oxygen carrier reactivity was first investigated. Figure 3 shows the reduction and oxidation reactivities for some carriers of NiO on  $\gamma\text{-Al}_2\text{O}_3$ ,  $\theta\text{-Al}_2\text{O}_3$  and  $\alpha\text{-Al}_2\text{O}_3$ . The Ni-based oxygen carrier impregnated on  $\gamma\text{-Al}_2\text{O}_3$  showed the lowest reactivity during the reduction reaction. On the contrary, the Ni-based oxygen carrier impregnated on  $\alpha\text{-Al}_2\text{O}_3$  showed the highest reactivity during the reduction reaction. All oxygen carriers exhibited very high reactivity during oxidation. It seems that the low reduction reactivity of the carrier of NiO on  $\gamma\text{-Al}_2\text{O}_3$  was due to the solid

state reaction between the NiO and the  $\gamma$ -Al<sub>2</sub>O<sub>3</sub> to form NiAl<sub>2</sub>O<sub>4</sub>, as it is shown in the XRD patterns (see Table 1). It must take into account that the reaction rate of CH<sub>4</sub> with NiAl<sub>2</sub>O<sub>4</sub> is lower than with free NiO. On the contrary, the high reactivity of the carrier of NiO on  $\alpha$ -Al<sub>2</sub>O<sub>3</sub> was because the interaction between the NiO and the support was reduced using the  $\alpha$ -Al<sub>2</sub>O<sub>3</sub>. As can be seen in Table 1, free NiO was observed in this oxygen carrier. The presence of an important fraction of active NiO was also visually confirmed because the oxygen carriers prepared with  $\alpha$ -Al<sub>2</sub>O<sub>3</sub> were green coloured against blue samples containing high fractions of NiAl<sub>2</sub>O<sub>4</sub>, as it was the case of the carriers prepared with  $\gamma$ -Al<sub>2</sub>O<sub>3</sub>.

Figure 4 shows the reduction and oxidation reactivities of the samples prepared by the deposition-precipitation method. The carrier prepared on  $\gamma$ -Al<sub>2</sub>O<sub>3</sub> by the deposition-precipitation method had higher reduction reactivity than the prepared by dry impregnation. However, the carriers prepared on  $\alpha$ -Al<sub>2</sub>O<sub>3</sub> by both methods showed more similar reactivities during reduction and oxidation reactions.

The amount of NiO and NiAl<sub>2</sub>O<sub>4</sub> was obtained in the TGA through TPR analysis using H<sub>2</sub> as reducing gas. Figure 5 shows the results of the H<sub>2</sub>-TPR analysis performed with the oxygen carriers after 5 reduction-oxidation cycles in the TGA. The TPR spectra shows a first weight loss in the temperature range of 400–600 °C and a second weight loss in the temperature range of 800-950 °C. The low temperature weight loss is well known to be due to the reduction of Ni<sup>2+</sup> in the NiO phase, whereas the high temperature weight loss is attributed to the reduction of Ni<sup>2+</sup> in the NiAl<sub>2</sub>O<sub>4</sub> spinel phase. In this sense, Figure 5 shows that the reduction of the oxygen carrier proceeded in two stages according to the reduction of the NiO at low temperature and NiAl<sub>2</sub>O<sub>4</sub> at high temperature, which was consistent with XRD data which indicated the presence of both NiO and NiAl<sub>2</sub>O<sub>4</sub> phases. It can be also observed that the fraction of oxygen carrier

reduced at low temperature, i.e. the fraction of free NiO, depended on the oxygen carrier. Comparing the results showed in Figure 5 and those showed in Figures 3 and 4 it is observed a good relationship between oxygen carrier reactivity and free NiO content in the oxygen carrier. The highest fraction of free NiO the highest reactivity.

### 3.2 Oxygen carrier behaviour in batch fluidized bed.

Reduction-oxidation multicycles with the Ni-based oxygen carriers were carried out in a batch fluidized bed reactor to determine the gas product distribution as a function of the operating conditions in similar conditions to that found in a CLR process and to analyze the fluidization behaviour of the oxygen carriers with respect to the carbon formation and agglomeration phenomena.

The main reactions happening with different contribution in a batch fluidized bed during the oxygen carrier reduction period are:

#### *Oxidation*



#### *Partial oxidation*



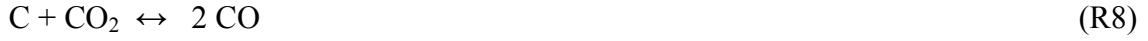
#### *Steam reforming catalyzed by Ni*



#### *Methane decomposition catalyzed by Ni*



*Carbon gasification*



*Water gas shift*



And during the oxygen carrier oxidation period:



The conversions of the oxygen carriers as function of time during the reduction and oxidation periods were calculated from the gas outlet concentrations by the equations:

*Reduction*

$$X_{red} = \int_{t_0}^{t_{red}} \frac{Q_{out}}{n_0 P_{tot}} (2P_{CO_2,out} + P_{CO,out} + P_{H_2O,out}) dt \quad (3)$$

$$Q_{out} = Q_{in} \left( \frac{P_{N_2,in}}{P_{N_2,out}} \right) = Q_{in} \left( \frac{P_{N_2,in}}{(1 - P_{CH_4,out} - P_{CO_2,out} - P_{CO,out} - P_{H_2,out} - P_{H_2O,out})} \right) \quad (4)$$

*Oxidation*

$$X_{oxi} = \int_{t_0}^{t_{oxi}} \frac{2Q_{out}}{n_0 P_{tot}} \left( \frac{Q_{in}}{Q_{out}} P_{O_2,in} - P_{O_2,out} - 1/2 P_{CO,out} - P_{CO_2,out} \right) dt \quad (5)$$

$$Q_{out} = \frac{Q_{in} (1 - P_{O_2,in})}{(1 - P_{CO_2,out} - P_{CO,out} - P_{O_2,out})} \quad (6)$$

where  $X$  is the conversion of the oxygen carrier,  $Q_{in}$  is the molar flow of the gas coming into the reactor,  $Q_{out}$  is the molar flow of the gas leaving the reactor,  $P_{tot}$  is the total pressure,  $P_{i,in}$  is the partial pressure of gas  $i$  incoming to the reactor,  $P_{i,out}$  is the partial pressure of gas  $i$  exiting the reactor,  $n_0$  are the moles of oxygen which can be removed from fully oxidized oxygen carrier, and  $t$  is the time.

The last terms in equation 5 take into account the formation of CO and CO<sub>2</sub> during the oxidation period due to the oxidation of C (reactions R11 and R12) coming from the decomposition of CH<sub>4</sub> (reaction R6) in the reduction period.

The back-mixing in the system, which was illustrated by the transient changes in gas concentration during the first seconds of reaction, was considered in order to obtain the actual concentration of the gases in the bed. The correction was done using a method of deconvolution, take into account for the distribution of the residence time of the gas in the system [13].

In the following sections the effect of the support, reaction temperature, H<sub>2</sub>O/CH<sub>4</sub> molar ratio, and preparation method on the gas product distribution and carbon formation is analyzed. For all the tests carried out in the batch fluidized bed total carbon, hydrogen and oxygen mass balances were done. The maximum deviations of the mass balances were  $\pm 6\%$  for C and  $\pm 4\%$  for H. All operating conditions were tested in the fluidized bed reactor for at least 10 cycles. Carbon deposited on the oxygen carrier was determined by integration of the CO<sub>2</sub> and CO generated during the oxidation reaction period. To determine the reduction period without carbon formation, different experiments were carried with decreasing reduction times. It was found that C deposited on the carrier increased with increasing the reduction time as it can be observed in Figures 6 and 7, which show the gas product distributions working with Ni11- $\alpha$ -Al<sub>2</sub>O<sub>3</sub> at 950 °C, H<sub>2</sub>O/CH<sub>4</sub>=0.3, during 5 and 7 minutes of reduction times. Figures 6 and 7 also

show the H<sub>2</sub>/CO molar ratio as a function of the time. It was found that the H<sub>2</sub>/CO molar ratio quickly increased when started the carbon formation, and the time without carbon formation corresponds to the points H<sub>2</sub>/CO<3. According with the set of reactions occurring during the reduction period (R1-R9) and for H<sub>2</sub>O/CH<sub>4</sub> molar ratios lower than 1, the H<sub>2</sub>/CO molar ratio should be lower than 3 if the H<sub>2</sub> is generated by reactions R4, R5 and R7. However, when reaction R6 occurs, there is carbon deposition on the carrier and a parallel decrease in the CO generation. As a consequence of the decrease in the CO generation the H<sub>2</sub>/CO molar ratio increases. Values of the H<sub>2</sub>/CO molar ratio higher than 3 indicated important carbon formation. This finding can be used to reduce the amount of experimental work because the carbon formation can be analyzed through the evolution of H<sub>2</sub>/CO molar ratio. Table 2 shows the rough reduction time without carbon deposition at different operating conditions using this criterion to determine the time for starting the carbon formation. The time without carbon formation during the reduction reaction depended on the oxygen carrier, temperature of operation, and H<sub>2</sub>O/CH<sub>4</sub> molar ratio.

### **3.2.1 Effect of support.**

$\gamma$ -Al<sub>2</sub>O<sub>3</sub>,  $\theta$ -Al<sub>2</sub>O<sub>3</sub> (obtained by calcination of  $\gamma$ -Al<sub>2</sub>O<sub>3</sub> at 1100 °C during 2 hours) and  $\alpha$ -Al<sub>2</sub>O<sub>3</sub> (obtained by calcination of  $\gamma$ -Al<sub>2</sub>O<sub>3</sub> at 1150 °C during 2 hours) particles were used as support to prepare oxygen carriers by dry impregnation (see Table 1). Figures 6 and 8 show the gas product distribution obtained, working at 950 °C and H<sub>2</sub>O/CH<sub>4</sub>=0.3, with the oxygen carriers prepared with the different supports.

With Ni-based oxygen carriers prepared on  $\gamma$ -Al<sub>2</sub>O<sub>3</sub> (Figure 8a), CO<sub>2</sub>, H<sub>2</sub>O, CO, and H<sub>2</sub> were formed almost immediately after introduction of CH<sub>4</sub> into the reactor. The CH<sub>4</sub>

conversion was complete, and high H<sub>2</sub> and CO concentrations were present in the gas outlet together with CO<sub>2</sub> and H<sub>2</sub>O during most of the reduction period. This behaviour indicated that the reduction process was mainly selective towards the formation of H<sub>2</sub> and CO.

With Ni-based oxygen carriers prepared on  $\alpha$ -Al<sub>2</sub>O<sub>3</sub> (Figure 6), CO<sub>2</sub> and H<sub>2</sub>O were formed immediately after the CH<sub>4</sub> feeding, and no CH<sub>4</sub> was detected during the whole carrier reduction time. During the first period, CO and H<sub>2</sub> concentration were those corresponding to the thermodynamic equilibrium at the reaction temperature. After that, CO<sub>2</sub> and H<sub>2</sub>O concentrations decreased, whereas the concentrations of CO and H<sub>2</sub> increased, indicating that the reduction process was mainly selective towards the formation of H<sub>2</sub> and CO. The change in the product selectivity during the reduction step is associated to changes in the catalyst degree of oxidation. At the beginning, the fully oxidized NiO favours the total oxidation of CH<sub>4</sub> (reactions R1-R3). As the sample was reduced, the selectivity of gas product formation changes from CO<sub>2</sub> and H<sub>2</sub>O to CO and H<sub>2</sub>, due to the occurrence of the CH<sub>4</sub> reforming and partial oxidation reactions (R4 and R5), catalyzed by reduced Ni active sites.

The oxygen carrier prepared on  $\theta$ -Al<sub>2</sub>O<sub>3</sub> (Figure 8b) showed the behaviour similar to the  $\alpha$ -Al<sub>2</sub>O<sub>3</sub>, but with this carrier the reduction time with almost complete conversion of CH<sub>4</sub> to CO<sub>2</sub> and H<sub>2</sub>O was smaller than with  $\alpha$ -Al<sub>2</sub>O<sub>3</sub>.

Zafar et al. [7] found significant amounts of unconverted CH<sub>4</sub> at the outlet the fuel reactor working with Cu-, Fe-, and Mn-based carriers, however, these authors found complete CH<sub>4</sub> conversion working with Ni-based oxygen carriers due to the catalytic effect of Ni on CH<sub>4</sub> pyrolysis. In our tests, the selectivity toward different gaseous products depended on the support used to prepare the Ni-based oxygen carrier, but with

the three supports the CH<sub>4</sub> conversion was complete, in good agreement with these authors.

During CH<sub>4</sub> reforming, as it is showed in Table 2, the reduction time without carbon deposition followed the order  $\gamma\text{-Al}_2\text{O}_3 > \theta\text{-Al}_2\text{O}_3 > \alpha\text{-Al}_2\text{O}_3$ . However, as a consequence of the different reactivity of the oxygen carriers (see Figure 3), the maximum conversions without carbon deposition reached by the oxygen carriers followed the order  $\alpha\text{-Al}_2\text{O}_3 > \theta\text{-Al}_2\text{O}_3 \approx \gamma\text{-Al}_2\text{O}_3$ . These results suggest that to obtain high H<sub>2</sub> and CO concentrations in a continuous CLC system the solid circulation rate and/or the solid inventory in the fuel reactor must be lower using the oxygen carrier prepared on  $\alpha\text{-Al}_2\text{O}_3$  than using the carriers prepared on  $\theta\text{-Al}_2\text{O}_3$  or  $\gamma\text{-Al}_2\text{O}_3$ .

Finally, it was found that all of the oxygen carriers showed a constant reaction rate during reduction and oxidation as a function of the number of the cycle, that is, deactivation was not observed. Similar results using MgAl<sub>2</sub>O<sub>4</sub> as support were found by Zafar et al. [7], however, these authors [6-7] using SiO<sub>2</sub> as support observed a clear decrease in the reactivity as a function of the number of cycles.

### **3.2.2 Effect of H<sub>2</sub>O/CH<sub>4</sub> molar ratio.**

Thermodynamic analyses show that in order to reach carbon free operation working with Ni-based oxygen carriers the O/C molar ratio must be higher than 1, being  $O/C = (O_{\text{H}_2\text{O}}/C) + (O_{\text{NiO}}/C)$ , where:  $O_{\text{H}_2\text{O}}$  = oxygen coming from the H<sub>2</sub>O and  $O_{\text{NiO}}$  = oxygen coming from the oxygen carrier. The  $O_{\text{NiO}}/C$  molar ratio depends on different factors, the most important being the oxygen carrier reactivity (that depends on the type of oxygen carrier, operating temperature,...) and the NiO content in the carrier. So, for a given temperature and oxygen carrier ( $O_{\text{NiO}}/C = \text{constant}$ ), an increase in the  $O_{\text{H}_2\text{O}}/C$



molar ratio increases the O/C molar ratio and decrease the carbon formation. If the O/C is lower than 1 and the reaction R4 (methane decomposition) is not produced, it is very obvious that at the exit of the fuel reactor unconverted methane should be measured.

The effect of the H<sub>2</sub>O/CH<sub>4</sub> molar ratio on the gas product distribution and carbon formation was analyzed with all the oxygen carriers prepared. Figures 9 and 10 show examples of the results obtained. As expected from thermodynamic analysis, for a given temperature, with all oxygen carriers, an increase in the H<sub>2</sub>O/CH<sub>4</sub> molar ratio produced an increase in the time of the reduction period without C deposition (see also Table 2). On the contrary, the maximum conversions of the oxygen carriers without C deposition were almost not affected by the H<sub>2</sub>O/CH<sub>4</sub> molar ratio. Figure 11 shows the H<sub>2</sub>/CO molar ratio in the gas product generated during CH<sub>4</sub> reforming. The H<sub>2</sub>/CO molar ratio was between 2 and 3 in most of the period without carbon formation, and this molar ratio increased to values higher than 3 when the C formation started. It was also observed that an increase in the H<sub>2</sub>O/CH<sub>4</sub> molar ratio produced a slight increase in the H<sub>2</sub>/CO molar ratio. These findings suggest that an increase of the H<sub>2</sub>O/CH<sub>4</sub> molar ratio increased the contribution of the steam reforming reaction (R5) and water gas shift (R9) in the global process and decreased the contributions of the partial oxidation (R4) and methane decomposition (R6).

### **3.2.3 Effect of reaction temperature.**

The effect of the reduction reaction temperature on the gas product distribution and carbon formation was analyzed with the different oxygen carriers prepared. Figure 12 shows the experimental results obtained with the oxygen carrier NiO<sub>21</sub>- $\gamma$ -Al<sub>2</sub>O<sub>3</sub>, working at four different temperatures between 800 and 950°C and a molar H<sub>2</sub>O/CH<sub>4</sub>

ratio of 0.3. It can be observed in the Figure 12, and also in the Table 2, that when the reduction reaction temperature increased the oxygen carrier conversion and the time of the reduction period without C formation increased significantly for all of the oxygen carriers. This is in agreement with the thermodynamic analysis because an increase in the operating temperature increases the oxygen carrier reactivity, and as a result increases the  $O_{NiO}/C$  molar ratio. At 950°C the carbon formation working with the oxygen carriers prepared by dry impregnation started when the oxygen carrier conversion was higher than 65-70%, even higher than 80% for the carrier NiO11- $\alpha$ Al<sub>2</sub>O<sub>3</sub>, however, this conversion decreased with decreasing the reduction reaction temperature.

Cho et al. [14] investigated for CLC the carbon formation of oxygen carriers based on nickel oxide and iron oxide. No carbon formation was found with oxygen carriers based on iron oxide. However, with the oxygen carriers based on nickel oxide these authors found that significant carbon formation started when the particles had lost so much oxygen that they were not able to convert much the fuel, and this was when 80% of oxygen had been consumed. The results obtained in our tests with the oxygen carrier NiO11- $\alpha$ Al<sub>2</sub>O<sub>3</sub> were similar to the results observed by Cho et al. [14]. However, it is clear that the conversion reached by the oxygen carrier before starting the carbon formation depended on their reactivity. As the reactivity increased with increasing the temperature, the carbon formation decreased with increasing the temperature.

### **3.2.4 Effect of preparation method.**

Two oxygen carriers, using  $\gamma$ -Al<sub>2</sub>O<sub>3</sub> and  $\alpha$ -Al<sub>2</sub>O<sub>3</sub> as supports, were also prepared by a deposition-precipitation method using urea. With this method a high active NiO content over the internal surface of the support was obtained in only one impregnation.

Figure 13 shows the gas product distributions obtained with these oxygen carriers. A comparison of these results with the results obtained with the oxygen carriers prepared by dry impregnation showed that the carriers prepared by dry impregnation had a reduction time period without carbon deposition longer than the oxygen carriers prepared by the deposition-precipitation method. In addition, the maximum oxygen carrier conversions without carbon deposition reached during the reduction period by the oxygen carriers prepared by the deposition-precipitation method were lower than those reached by the oxygen carriers prepared by dry impregnation. At 950 °C the deposition of C with the NiO28- $\gamma$ Al<sub>2</sub>O<sub>3</sub> and NiO26- $\alpha$ Al<sub>2</sub>O<sub>3</sub> oxygen carriers started at oxygen carrier conversions of 20-35% and 25-35% respectively. These conversions were significantly lower than those obtained with the carriers NiO21- $\gamma$ Al<sub>2</sub>O<sub>3</sub> and NiO11- $\alpha$ Al<sub>2</sub>O<sub>3</sub>, ~75% and ~85% respectively. However, it is not clear why the oxygen carriers prepared by the deposition-precipitation method had a higher tendency to increase the carbon formation because the reactivity of these carriers was similar or even higher than the reactivity of the oxygen carriers prepared by dry impregnation.

#### **4. Conclusions.**

The Ni-based oxygen carrier impregnated on  $\gamma$ -Al<sub>2</sub>O<sub>3</sub> showed the lowest reactivity during the reduction reaction. On the contrary, the Ni-based oxygen carrier impregnated on  $\alpha$ -Al<sub>2</sub>O<sub>3</sub> showed the highest reactivity during the reduction reaction. All oxygen carriers exhibited very high reactivity during oxidation. The low reduction reactivity of

the carrier of NiO on  $\gamma$ -Al<sub>2</sub>O<sub>3</sub> was due to the solid state reaction between the NiO and the  $\gamma$ -Al<sub>2</sub>O<sub>3</sub> to form NiAl<sub>2</sub>O<sub>4</sub>. The high reduction reactivity of the carrier of NiO on  $\alpha$ -Al<sub>2</sub>O<sub>3</sub> was because the interaction between the NiO and the support was reduced using the  $\alpha$ -Al<sub>2</sub>O<sub>3</sub>.

The carrier prepared on  $\gamma$ -Al<sub>2</sub>O<sub>3</sub> by the deposition-precipitation method had higher reduction reactivity than the prepared by dry impregnation. However, the carriers prepared on  $\alpha$ -Al<sub>2</sub>O<sub>3</sub> by both methods showed similar reactivities during reduction and oxidation reactions.

The test carried out in the batch fluidized bed showed that Ni-based oxygen carriers prepared by dry impregnation on  $\gamma$ -Al<sub>2</sub>O<sub>3</sub>,  $\theta$ -Al<sub>2</sub>O<sub>3</sub>, and  $\alpha$ -Al<sub>2</sub>O<sub>3</sub> are suitable for autothermal reforming of methane during long periods of time without carbon deposition. On the contrary, the oxygen carriers prepared by a deposition-precipitation method using urea had a higher tendency to increase the C formation.

For all of the oxygen carriers, the reduction time without carbon deposition increased with increasing the reduction reaction temperature and the H<sub>2</sub>O/CH<sub>4</sub> molar ratio in the feed. Working at temperatures of 950 °C and H<sub>2</sub>O/CH<sub>4</sub> molar ratios of 0.3-0.7, with the oxygen carriers Ni21- $\gamma$ Al<sub>2</sub>O<sub>3</sub>, Ni16- $\theta$ Al<sub>2</sub>O<sub>3</sub> and Ni11  $\alpha$ Al<sub>2</sub>O<sub>3</sub>, the carbon deposition started when the oxygen carrier conversions were higher than 60-70%. However this value decreased when the temperature decreased.

The H<sub>2</sub>/CO molar ratio in the gas product generated during CH<sub>4</sub> reforming was between 2 and 3 in the period without carbon formation. This molar ratio increased to values higher than 3 when the C formation started.

## **Acknowledgments**

This work was partially supported by the European Commission, under the 6th Framework Programme (CACHET Project, Contract no. 019972), and from the CCP2 (CO<sub>2</sub> Capture Project), a partnership of BP, Chevron, Conoco-Phillips, Eni Technology, Norsk Hydro, Shell, Suncor, and Petrobras. M. Ortiz thanks Diputación General de Aragón for the F.P.I. fellowship.

## References

- [1] I. Dybkær. Tubular reforming and autothermal reforming of natural gas - an overview of available processes. *Fuel Proc. Technol.* 42 (1995), 85-107.
- [2] J.R. Rostrup-Nielsen. Production of synthesis gas. *Catal. Today* 18 (1993), 305-324.
- [3] J.H. Edwards, A.M. Maitra. The chemistry of methane reforming with carbon dioxide and its current and potential applications. *Fuel Proc. Technol.* 42 (1995), 269-289.
- [4] T. Mattisson, A. Lyngfelt. Applications of chemical-looping combustion with capture of CO<sub>2</sub>. *Proceedings of the 2<sup>th</sup> Nordic Minisymposium on Carbon Dioxide Capture and Storage*, Göteborg, Sweden , 2001.
- [5] T. Mattisson, Q. Zafar, A. Lyngfelt, B. Gevert. Integrated hydrogen and power production from natural gas with CO<sub>2</sub> capture. *15th World Hydrogen Energy Conference*, Yokohama, Japan , 2004.
- [6] Q. Zafar, T. Mattisson , B. Gevert. Integrated hydrogen and power production with CO<sub>2</sub> capture using chemical-looping reforming-Redox reactivity of particles of CuO, Mn<sub>2</sub>O<sub>3</sub>, NiO, and Fe<sub>2</sub>O<sub>3</sub> using SiO<sub>2</sub> as a support. *Ind. Eng. Chem. Res.* 44 (2005), 3485-3498.

- [7] Q. Zafar, T. Mattisson, B. Gevert. Redox investigation of some oxides of transition-state metals Ni, Cu, Fe and Mn supported on SiO<sub>2</sub> and MgAl<sub>2</sub>O<sub>4</sub>, *Energy Fuels* 20 (2006), 34-44.
- [8] M. Ryden, A. Lyngfelt, T. Mattisson. Synthesis gas generation by chemical-looping reforming in a continuously operating laboratory reactor. *Fuel* 85 (2006), 1631-1641.
- [9] H. Zhao, D.J. Draelants, G. V. Baron. Preparation and characterisation of nickel-modified ceramic filters. *Catal. Today* 56 (2000) 229-237.
- [10] J.W. Geus and A.J. Van Dillen, 1997. In *Handbook of Heterogeneous Catalysis*, Vol. 1. Ed. Ertl, G., Knözinger, H., and Weitkamp, J., WILEY-VCH.
- [11] J. Adánez, L.F. de Diego, F. García-Labiano, P. Gayán, A. Abad and J.M. Palacios. Selection of Oxygen Carriers for Chemical-Looping Combustion. *Energy Fuels* 18 (2004), 371-377
- [12] L.F. de Diego, F. García-Labiano, J. Adánez, P. Gayán, A. Abad, B.M. Corbella and J.M. Palacios. Development of Cu-based oxygen carriers for chemical-looping combustion. *Fuel* 83 (2004), 1749-1757
- [13] Levenspiel O. *Chemical Reaction Engineering*. New York: John Willey and Sons; 1981.
- [14] P. Cho, T. Mattisson, A. Lyngfelt. Carbon formation on nickel and iron oxide-containing oxygen carriers for chemical-looping combustion. *Ind. Eng. Chem. Res.* 44 (2005), 668-676.

## Captions for the Figures

Figure 1. Chemical-Looping Reforming.

Figure 2. Experimental setup used for multicycle tests in a batch fluidized bed reactor.

Figure 3. Reactivity in TGA of Ni-based oxygen carriers prepared by dry impregnation on different supports.  $T=950^{\circ}\text{C}$ .

Figure 4. Effect of the preparation method on the reactivity of the oxygen carriers.  $T=950^{\circ}\text{C}$ .

Figure 5. Behaviour of the oxygen carriers during temperature programmed reduction tests in TGA. Reducing gas: 10 vol.% of  $\text{H}_2$  in Ar.

Figure 6. Gas product distribution and  $\text{H}_2/\text{CO}$  molar ratio in a test with a reduction time of 5 min.  $\text{NiO}_{11-\alpha}\text{Al}_2\text{O}_3$ .  $\text{H}_2\text{O}/\text{CH}_4=0.3$ ,  $T=950^{\circ}\text{C}$ .

Figure 7. Gas product distribution and  $\text{H}_2/\text{CO}$  molar ratio in a test with a reduction time of 7 min.  $\text{NiO}_{11-\alpha}\text{Al}_2\text{O}_3$ .  $\text{H}_2\text{O}/\text{CH}_4=0.3$ ,  $T=950^{\circ}\text{C}$ .

Figure 8. Effect of support on the gas product distribution and oxygen carrier conversion. a)  $\text{NiO}_{21-\gamma}\text{Al}_2\text{O}_3$ , b)  $\text{NiO}_{16-\theta}\text{Al}_2\text{O}_3$ .  $\text{H}_2\text{O}/\text{CH}_4=0.3$ ,  $T=950^{\circ}\text{C}$ .

Figure 9. Effect of  $\text{H}_2\text{O}/\text{CH}_4$  molar ratio on the gas product distribution and oxygen carrier conversion.  $\text{NiO}_{11-\alpha}\text{Al}_2\text{O}_3$ ,  $T=950^{\circ}\text{C}$ . a)  $\text{H}_2\text{O}/\text{CH}_4=0.5$ , b)  $\text{H}_2\text{O}/\text{CH}_4=0.7$ .

Figure 10. Effect of  $\text{H}_2\text{O}/\text{CH}_4$  molar ratio on the gas product distribution and oxygen carrier conversion.  $\text{NiO}_{21-\gamma}\text{Al}_2\text{O}_3$ ,  $T=950^{\circ}\text{C}$ . a)  $\text{H}_2\text{O}/\text{CH}_4=0.5$ , b)  $\text{H}_2\text{O}/\text{CH}_4=0.7$ .

Figure 11. Effect of  $\text{H}_2\text{O}/\text{CH}_4$  molar ratio on the  $\text{H}_2/\text{CO}$  molar ratio.  $\text{NiO}_{21-\gamma}\text{Al}_2\text{O}_3$ ,  $T=950^{\circ}\text{C}$ . a)  $\text{NiO}_{21-\gamma}\text{Al}_2\text{O}_3$ , b)  $\text{NiO}_{11-\alpha}\text{Al}_2\text{O}_3$ .  $T=950^{\circ}\text{C}$ .

Figure 12. Effect of reduction reaction temperature on the gas product distribution and oxygen carrier conversion. NiO21- $\gamma$ Al<sub>2</sub>O<sub>3</sub>, H<sub>2</sub>O/CH<sub>4</sub>=0.3.

Figure 13. Gas product distributions and oxygen carrier conversions obtained with the oxygen carriers prepared by the deposition-precipitation method. a) Ni28- $\gamma$ Al<sub>2</sub>O<sub>3</sub>, b) Ni26- $\alpha$ Al<sub>2</sub>O<sub>3</sub>. T=950°C, H<sub>2</sub>O/CH<sub>4</sub>=0.7.



**Table 1.** Physical properties and solid composition of the oxygen carriers.

Oxygen carrier	Preparation method (*)	Density	Porosity	Crushing strength	XRD
		g /cm <sup>3</sup>	%	N	
NiO21- $\gamma$ Al <sub>2</sub> O <sub>3</sub>	Dry impregnation (2)	1.7	50.7	2.6	$\gamma$ -Al <sub>2</sub> O <sub>3</sub> , NiAl <sub>2</sub> O <sub>4</sub>
NiO16- $\theta$ Al <sub>2</sub> O <sub>3</sub>	Dry impregnation (2)	2.0	48.6	3.3	$\alpha$ -Al <sub>2</sub> O <sub>3</sub> , NiAl <sub>2</sub> O <sub>4</sub> , NiO
NiO11- $\alpha$ Al <sub>2</sub> O <sub>3</sub>	Dry impregnation (2)	2.3	42.9	5.2	$\alpha$ -Al <sub>2</sub> O <sub>3</sub> , NiO, NiAl <sub>2</sub> O <sub>4</sub>
NiO28 - $\gamma$ Al <sub>2</sub> O <sub>3</sub>	Precipitation-deposition	1.8	46.5	2.3	$\gamma$ -Al <sub>2</sub> O <sub>3</sub> , NiAl <sub>2</sub> O <sub>4</sub> , NiO
NiO26- $\alpha$ Al <sub>2</sub> O <sub>3</sub>	Precipitation-deposition	2.6	41.5	5.1	$\alpha$ -Al <sub>2</sub> O <sub>3</sub> , NiO, NiAl <sub>2</sub> O <sub>4</sub>

(\*) In bracket the number of impregnations carried out for the oxygen carrier preparation.

**Table 2.** Operating conditions used in the batch fluidized bed experimental tests and rough time and oxygen carrier conversion without carbon deposition.

Oxygen carrier	Temperature (°C)	H <sub>2</sub> O/CH <sub>4</sub> molar ratio	Rough time without carbon deposition (minutes)	Maximum oxygen carrier conversion without carbon deposition (%)
NiO11- $\alpha$ Al <sub>2</sub> O <sub>3</sub>	950	0.3	5	89±3
		0.5	6	89±4
		0.7	8	85±5
NiO11- $\alpha$ Al <sub>2</sub> O <sub>3</sub>	800	0.3	1.5	52±3
		0.5	2	55±5
		0.7	3	57±4
NiO16- $\theta$ Al <sub>2</sub> O <sub>3</sub>	950	0.3	5	65±2
		0.5	7	67±3
		0.7	8	68±5
NiO16- $\theta$ Al <sub>2</sub> O <sub>3</sub>	800	0.3	1	21±3
		0.5	1.25	21±2
		0.7	1.5	23±4
NiO21- $\gamma$ Al <sub>2</sub> O <sub>3</sub>	950	0.3	9	77±4
		0.5	12	76±4
		0.7	17	70±7
NiO21- $\gamma$ Al <sub>2</sub> O <sub>3</sub>	800	0.3	3	20±3
		0.5	5	20±4
		0.7	7	24±4
NiO21- $\gamma$ Al <sub>2</sub> O <sub>3</sub>	850	0.3	5	30±3
NiO21- $\gamma$ Al <sub>2</sub> O <sub>3</sub>	900	0.3	7	58±4
NiO28- $\gamma$ Al <sub>2</sub> O <sub>3</sub>	950	0.3	< 1	20±6
		0.5	1	22±4
		0.7	3	35±6
NiO26- $\alpha$ Al <sub>2</sub> O <sub>3</sub>	950	0.3	<1	25±4
		0.5	<1.5	30±5
		0.7	<2.5	35±6

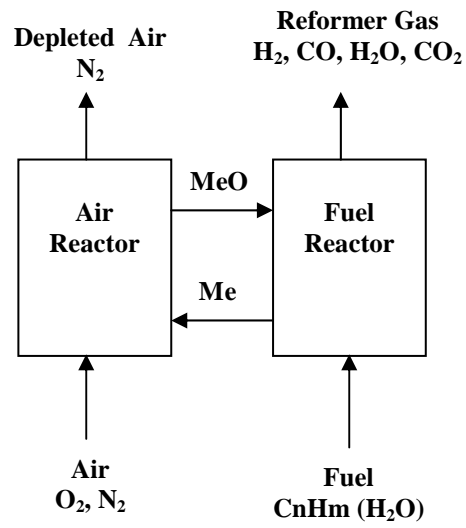


Figure 1. Chemical-Looping Reforming.

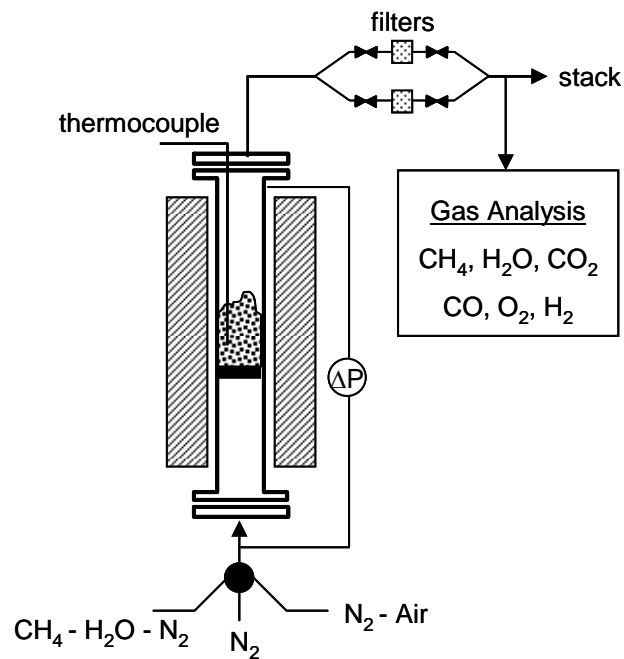


Figure 2. Experimental setup used for multicycle tests in a batch fluidized bed reactor.

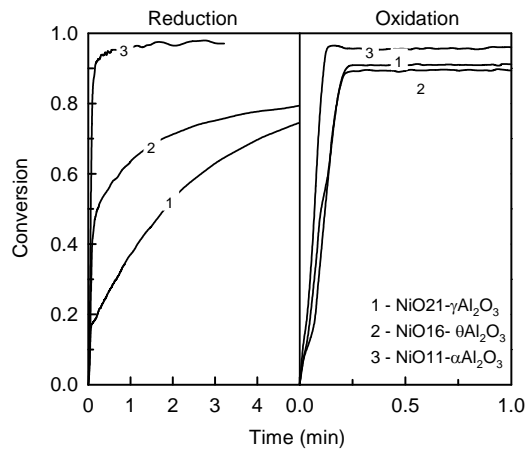


Figure 3. Reactivity in TGA of Ni-based oxygen carriers prepared by dry impregnation on different supports. T=950°C

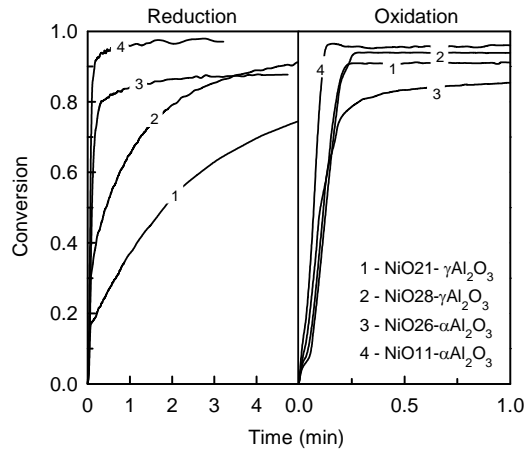


Figure 4. Effect of the preparation method on the reactivity of the oxygen carriers. T=950°C.

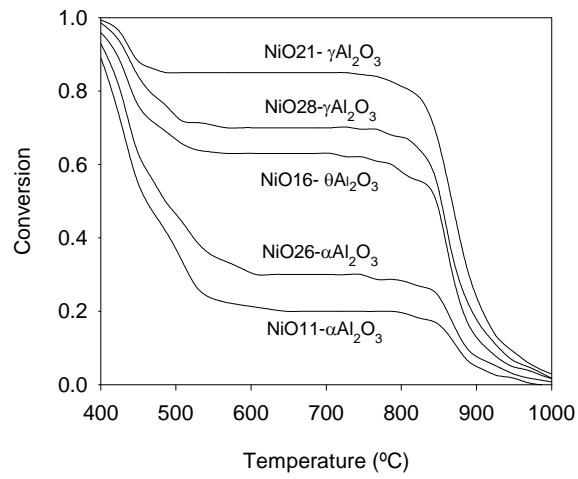


Figure 5. Behaviour of the oxygen carriers during temperature programmed reduction tests in TGA. Reducing gas: 10 vol.% of H<sub>2</sub> in Ar.

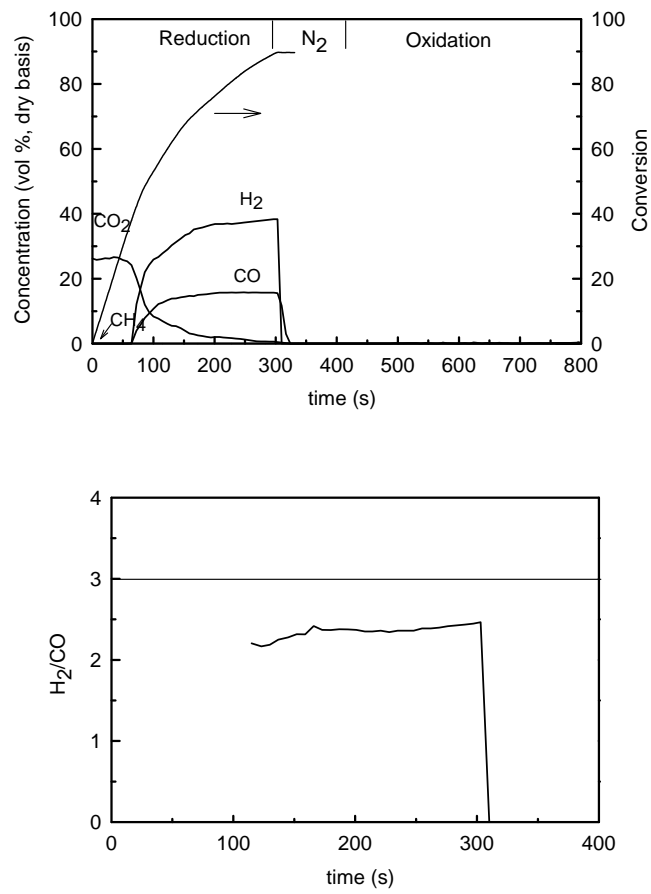


Figure 6. Gas product distribution and H<sub>2</sub>/CO molar ratio in a test with a reduction time of 5 min. NiO11- $\alpha$ Al<sub>2</sub>O<sub>3</sub>. H<sub>2</sub>O/CH<sub>4</sub>=0.3, T=950°C.

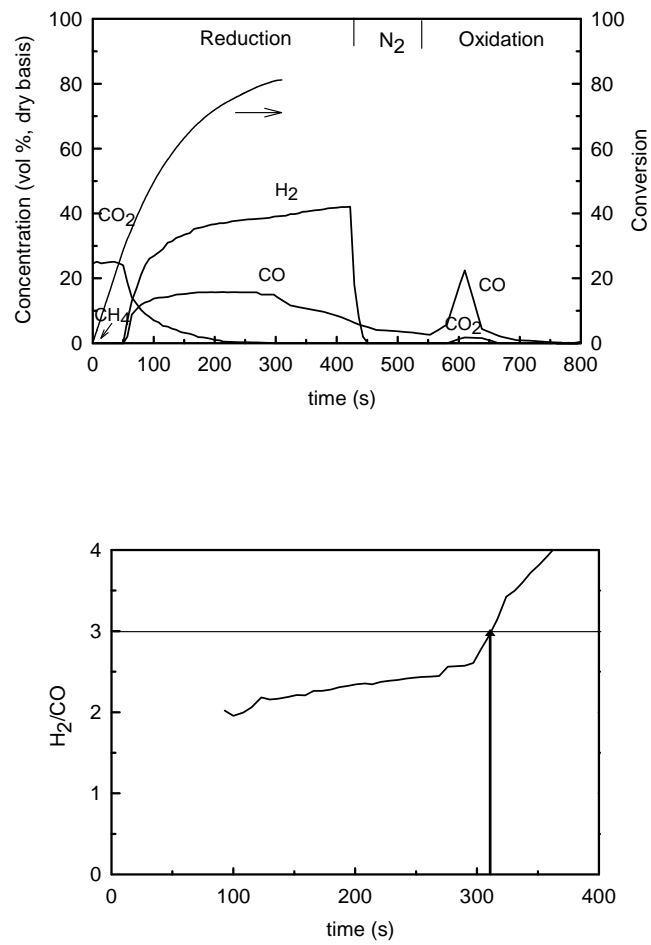


Figure 7. Gas product distribution and H<sub>2</sub>/CO molar ratio in a test with a reduction time of 7 min. NiO11- $\alpha$ Al<sub>2</sub>O<sub>3</sub>. H<sub>2</sub>O/CH<sub>4</sub>=0.3, T=950°C.

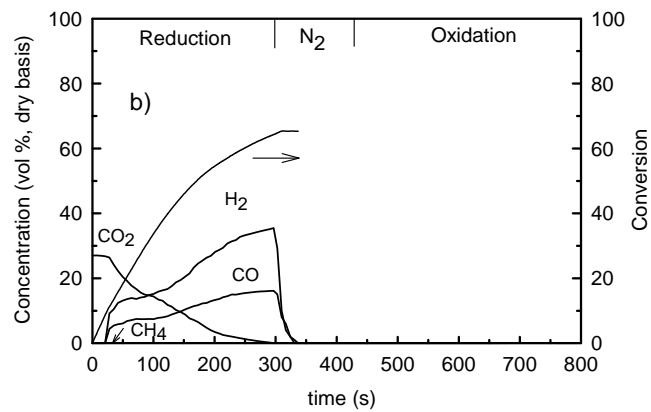
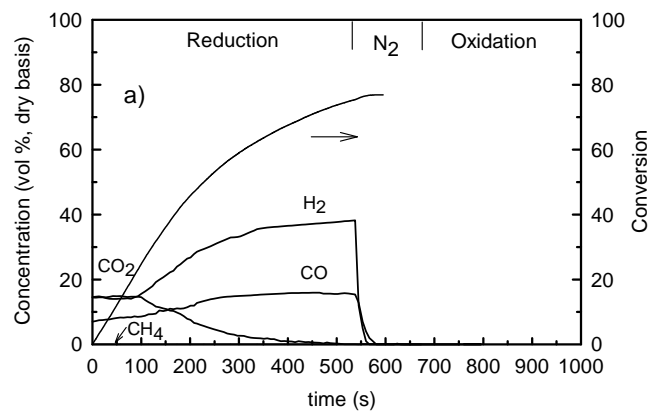


Figure 8. Effect of support on the gas product distribution and oxygen carrier conversion. a) NiO<sub>21</sub>- $\gamma$ -Al<sub>2</sub>O<sub>3</sub>, b) NiO<sub>16</sub>- $\theta$ -Al<sub>2</sub>O<sub>3</sub>. H<sub>2</sub>O/CH<sub>4</sub>=0.3, T=950°C.



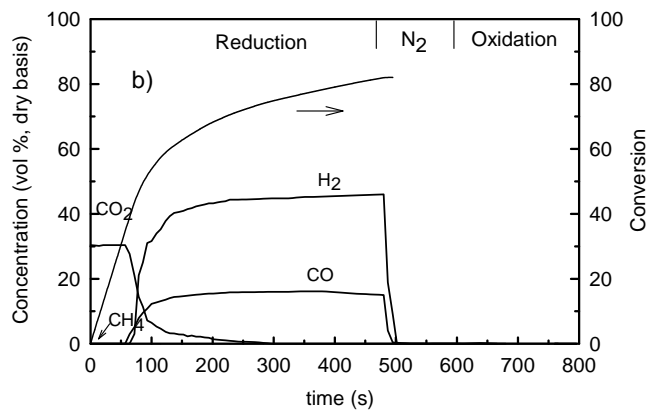
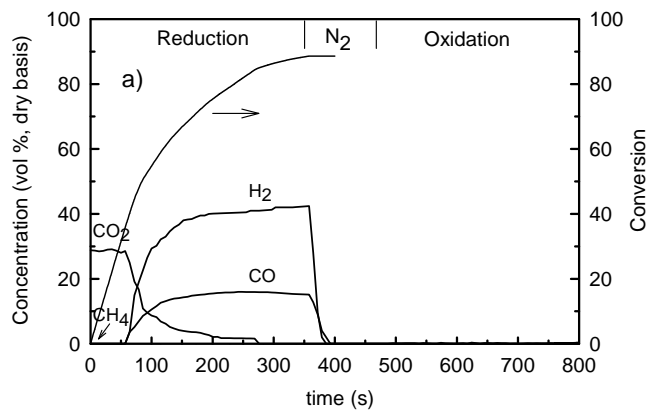


Figure 9. Effect of  $\text{H}_2\text{O}/\text{CH}_4$  molar ratio on the gas product distribution and oxygen carrier conversion.  $\text{NiO}_{1-\alpha}\text{Al}_2\text{O}_3$ ,  $T=950^\circ\text{C}$ . a)  $\text{H}_2\text{O}/\text{CH}_4=0.5$ , b)  $\text{H}_2\text{O}/\text{CH}_4=0.7$ .

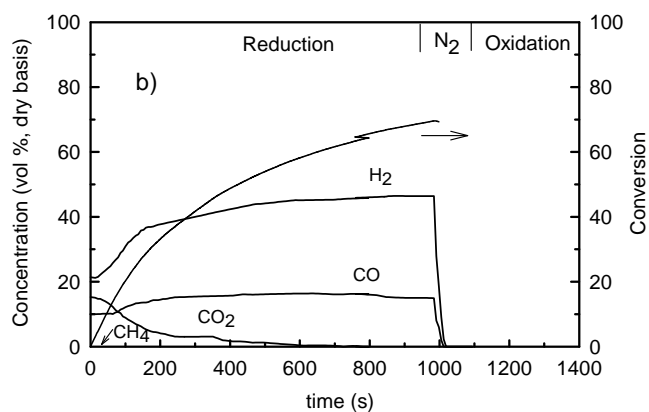
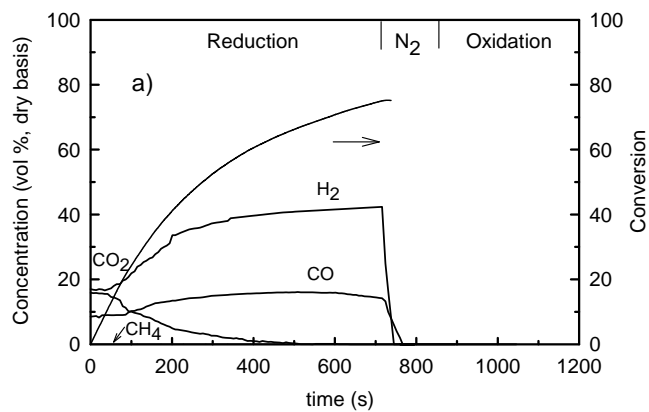


Figure 10. Effect of  $\text{H}_2\text{O}/\text{CH}_4$  molar ratio on the gas product distribution and oxygen carrier conversion.  $\text{NiO}_{21-\gamma}\text{Al}_2\text{O}_3$ ,  $T=950^\circ\text{C}$ . a)  $\text{H}_2\text{O}/\text{CH}_4=0.5$ , b)  $\text{H}_2\text{O}/\text{CH}_4=0.7$ .

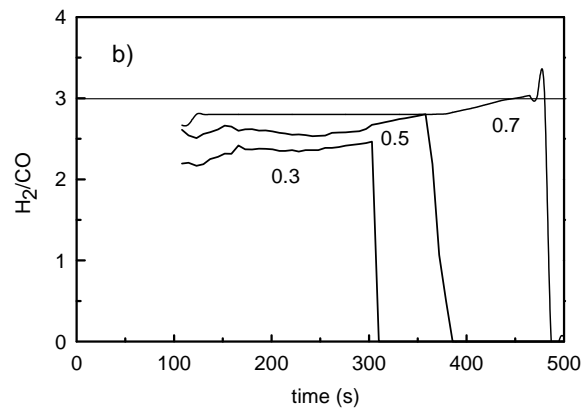
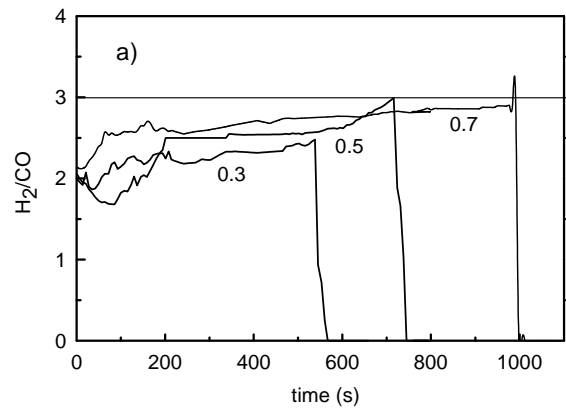


Figure 11. Effect of  $\text{H}_2\text{O}/\text{CH}_4$  molar ratio on the  $\text{H}_2/\text{CO}$  molar ratio.  $\text{NiO}_{21}\text{-}\gamma\text{Al}_2\text{O}_3$ ,  $T=950^\circ\text{C}$ . a)  $\text{NiO}_{21}\text{-}\gamma\text{Al}_2\text{O}_3$ , b)  $\text{NiO}_{11}\text{-}\alpha\text{Al}_2\text{O}_3$ .  $T=950^\circ\text{C}$ .

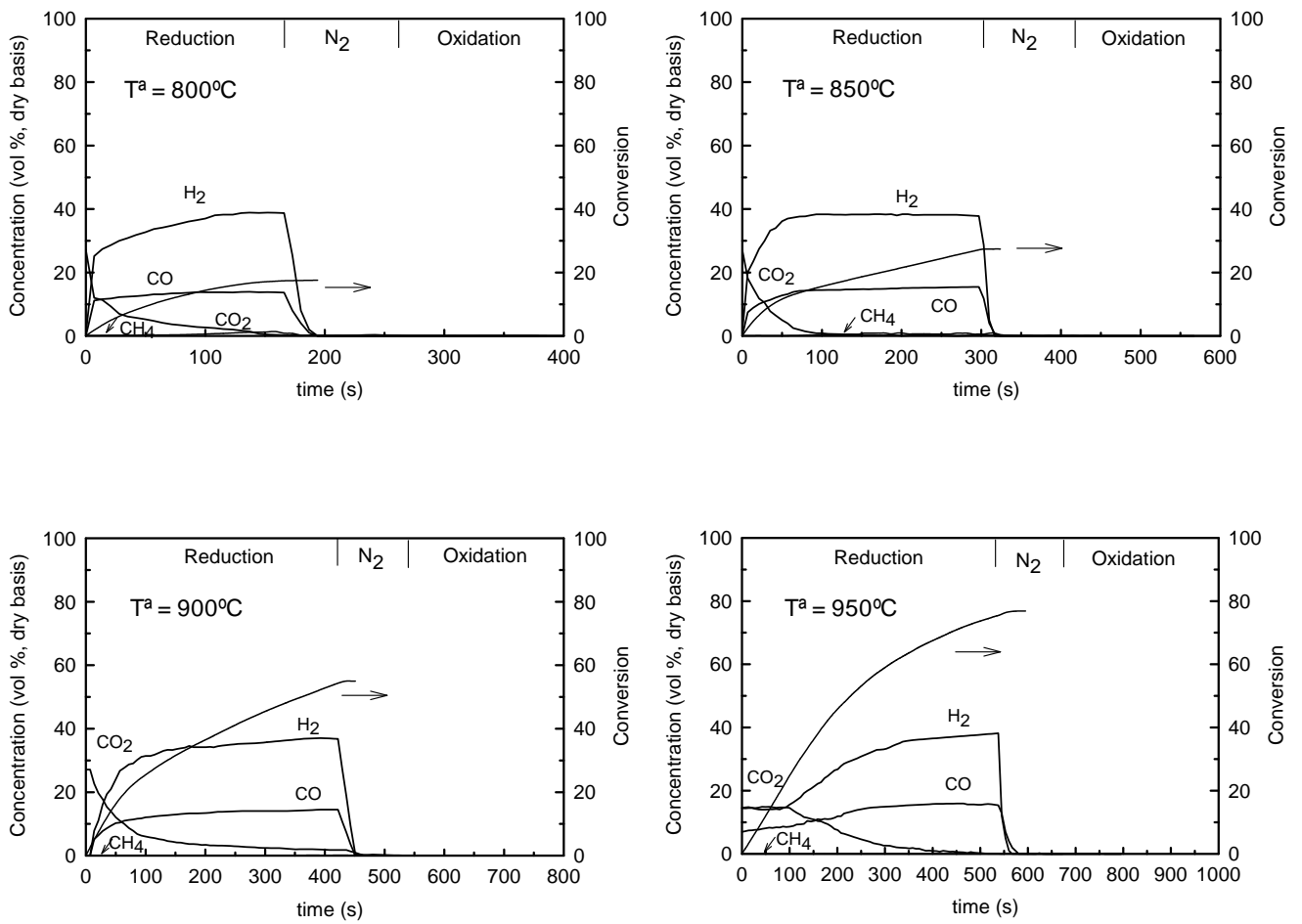


Figure 12. Effect of reduction reaction temperature on the gas product distribution and oxygen carrier conversion. NiO<sub>2</sub>1- $\gamma$ Al<sub>2</sub>O<sub>3</sub>, H<sub>2</sub>O/CH<sub>4</sub>=0.3.

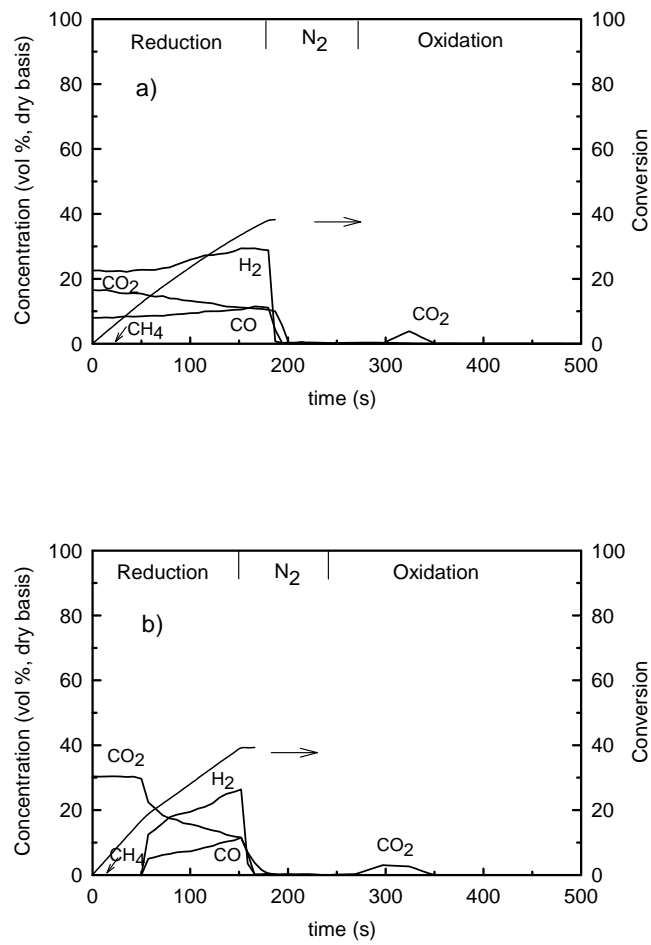


Figure 13. Gas product distributions and oxygen carrier conversions obtained with the oxygen carriers prepared by the deposition-precipitation method. a) Ni<sub>28</sub>- $\gamma$ -Al<sub>2</sub>O<sub>3</sub>, b) Ni<sub>26</sub>- $\alpha$ -Al<sub>2</sub>O<sub>3</sub>. T=950°C, H<sub>2</sub>O/CH<sub>4</sub>=0.7.